Naval Information Warfare Center PACIFIC

TECHNICAL REPORT 3337
FEBRUARY 2024

Towards Pulsed Laser Deposition of 2D Materials and Cryogenic Photoluminescence Spectroscopy of 2D Transition Metal Dichalcogenides

Carlos M. Torres Jr.
Alexandru Hening
Melvin Pascoguin
James R. Adleman

NIWC Pacific

Naval Information Warfare Center (NIWC) Pacific
San Diego, CA 92152-5001

This page is intentionally blank.

TECHNICAL REPORT 3337
FEBRUARY 2024

Towards Pulsed Laser Deposition of 2D Materials and Cryogenic Photoluminescence Spectroscopy of 2D Transition Metal Dichalcogenides

Carlos M. Torres Jr.
Alexandru Hening
Melvin Pascoguin
James Adleman

NIWC Pacific

Administrative Notes:
This report was approved through the Release of Scientific and Technical Information (RSTI) process in October 2023 and formally published in the Defense Technical Information Center (DTIC) in February 2024.

NIWC Pacific
San Diego, CA 92152-5001

NIWC Pacific
San Diego, California 92152-5001

P. M. McKenna, CAPT, USN
Commanding Officer

M. J. McMillan
Executive Director

ADMINISTRATIVE INFORMATION

The work described in this report was performed by scientists and engineers in the Advanced Photonic Technologies Branch (Code 55360) of the Enterprise Communications and Networks Division/Communications and Networks Department, Naval Information Warfare Center (NIWC) Pacific, San Diego, CA. The NIWC Pacific Naval Innovative Science and Engineering (NISE) Program as well as the Office of Naval Research (ONR) provided funding for these Basic Research projects.

Released by
Brent Murray, Division Head
Enterprise Communications and Networks

Under authority of
Susie Hartzog, Department Head
Communications and Networks

ACKNOWLEDGMENTS

This work would not have been possible without the generous financial support from the NIWC Pacific NISE Program and the ONR during the FY21–23 Basic Research efforts.

Editor: MGK

EXECUTIVE SUMMARY

This technical report summarizes the work executed during FY21–FY23 of the Office of Naval Research (ONR)-funded Electrically-Tunable On-Demand Energy Bandstructures in Pulse Laser Deposited 2D Quantum Material Heterostructure-Based Devices (Qu-PLD) project and during FY21–FY22 of the Naval Information Warfare Center (NIWC) Pacific Naval Innovative Science and Engineering (NISE)-funded Quantum Engineered Nanodevices Exploiting Twistronics for Electromagnetic Maneuver Warfare (EMW) and Command, Control, Communications, Computers, Intelligence, Surveillance, and Reconnaissance (C4ISR) project. Most of the work was performed by NIWC Pacific scientists and engineers in the Quantum Engineered Nano Devices Laboratory (QENDL) at NIWC Pacific in San Diego, CA.

This page is intentionally blank.

ACRONYMS

2D	two-dimensional
C5ISRT	Command, Control, Computers, Communications, Cyber, Intelligence, Surveillance, Reconnaissance, and Targeting
COTS	commercial off-the-shelf
CVD	Chemical vapor deposition
DC	direct current
DOE	design of experiments
DON	Department of the Navy
DPSSL	diode-pumped solid-state laser
EMW	Electromagnetic Maneuver Warfare
FTIR	Fourier transform infrared
FWHM	full width at half maximum
KrF	krypton fluoride
MBE	molecular beam epitaxy
MMF	multi-mode fiber
MOS2	molybdenum disulfide
MOSE2	molybdenum diselenide
NIWC Pacific	Naval Information Warfare Center Pacific
NSWC Crane	Naval Surface Warfare Center, Crane Division
ONR	Office of Naval Research
PL	photoluminescence
PLD	pulsed laser deposition
QENDL	Quantum Engineered Nano Devices Laboratory
RDT&E	Research, development, test, and evaluation
SMF	single-mode fiber
TMDs	transition metal dichalcogenides
WS2	tungsten disulfide
WSE2	tungsten diselenide
XRD	x-ray diffraction
XRR	x-ray reflectivity

This page is intentionally blank.

CONTENTS

FIGURES

TABLES

1. INTRODUCTION

The Conceptual Vision of the Operational Battlespace of 2045 in the 2017 Department of the Navy's (DON) 30 Year Research and Development Plan predicts quantum-based sensing, nanotechnology, and photonics as key programs and technology investments [1]. The DON identifies advanced materials and manufacturing technologies and advanced computing and sensing as core technology areas that must be built and sustained. The Electromagnetic Maneuver Warfare (EMW) focus area in the 2015 Office of Naval Research's (ONR) Naval Science and Technology Strategy seeks to "enable the warfighter to have complete control over the electromagnetic spectrum…" [2]. Furthermore, the 2023 National Defense Science and Technology Strategy identifies quantum science, advanced materials, and microelectronics as critical technology areas and mentions that "We must make foundational investments in the equipment and facilities required to discover and test new capabilities… Not only will these investments introduce new capabilities to our infrastructure, they will also help attract and retain the most sought-after talent." [3].

For these reasons, the Naval Information Warfare Center (NIWC) Pacific continues to invest in maintaining a state-of-the-art laboratory, the Quantum Engineered Nano Devices Laboratory (QENDL) [4], which emphasizes various modalities of characterization of advanced materials and devices. QENDL's mission is to explore and exploit the exotic properties of atomic-layered two-dimensional (2D) materials, quantum materials, and their heterostructures for the benefit of the future warfighter in terms of command, control, computers, communications, cyber, intelligence, surveillance, reconnaissance, and targeting (C5ISRT), EMW, and spectrum dominance.

This technical report summarizes most of the work [5–7] executed during FY21–FY23 of the ONR-funded Electrically-Tunable On-Demand Energy Bandstructures in Pulse Laser Deposited (PLD) 2D Quantum Material Heterostructure-Based Devices (Qu-PLD) project and during FY21–FY22 of the NIWC Pacific Naval Innovative Science and Engineering (NISE)-funded Quantum Engineered Nanodevices Exploiting Twistronics for EMW and Command, Control, Communications, Computers, Intelligence, Surveillance, and Reconnaissance (C4ISR) project. The ONR project investigated developing a rapid, scalable, and high-throughput method to synthesize continuous large-area 2D semiconductors on arbitrary substrates using PLD of multiple materials without breaking chamber vacuum, thus leading to higher-quality heterointerfaces compared to the state-of-the-art (i.e., dry transfer of micron-sized mechanically exfoliated flakes from bulk crystals or wet transfer of chemical vapor deposition (CVD) 2D materials). The ONR and NISE projects also focused on establishing a novel fiber-optic-based cryogenic photoluminescence (PL) spectroscopy setup for rapid prototyping of 2D materials prior to their incorporation into devices.

This page is intentionally blank.

2. BACKGROUND

Pulsed laser deposition (PLD) was performed at NIWC Pacific using a PVD Products Nano-PLD chamber; see Figure 1. This chamber accommodates 6 (1-inch) ablation targets on a carousel, and the targets were procured from either Stanford Advanced Materials or Plasmaterials, Inc. The various PLD parameters to investigate in our design of experiments (DOE) include excimer laser fluence, excimer laser repetition rate, substrate temperature, substrate rotation speed, target rotation speed, substrate (i.e., sapphire (0001)), gas species in the chamber during deposition, target-to-substrate distance, background (process) pressure in the chamber, etc. Our PLD system is shown in the images on the right side of the figure. A 248nm krypton fluoride (KrF) excimer laser is routed via an optical train into the PLD vacuum chamber and ablates a selected material target that produces an energetic plasma plume that stoichiometrically deposits the material onto a heated 2-inch substrate some distance away normal to the ablation target.

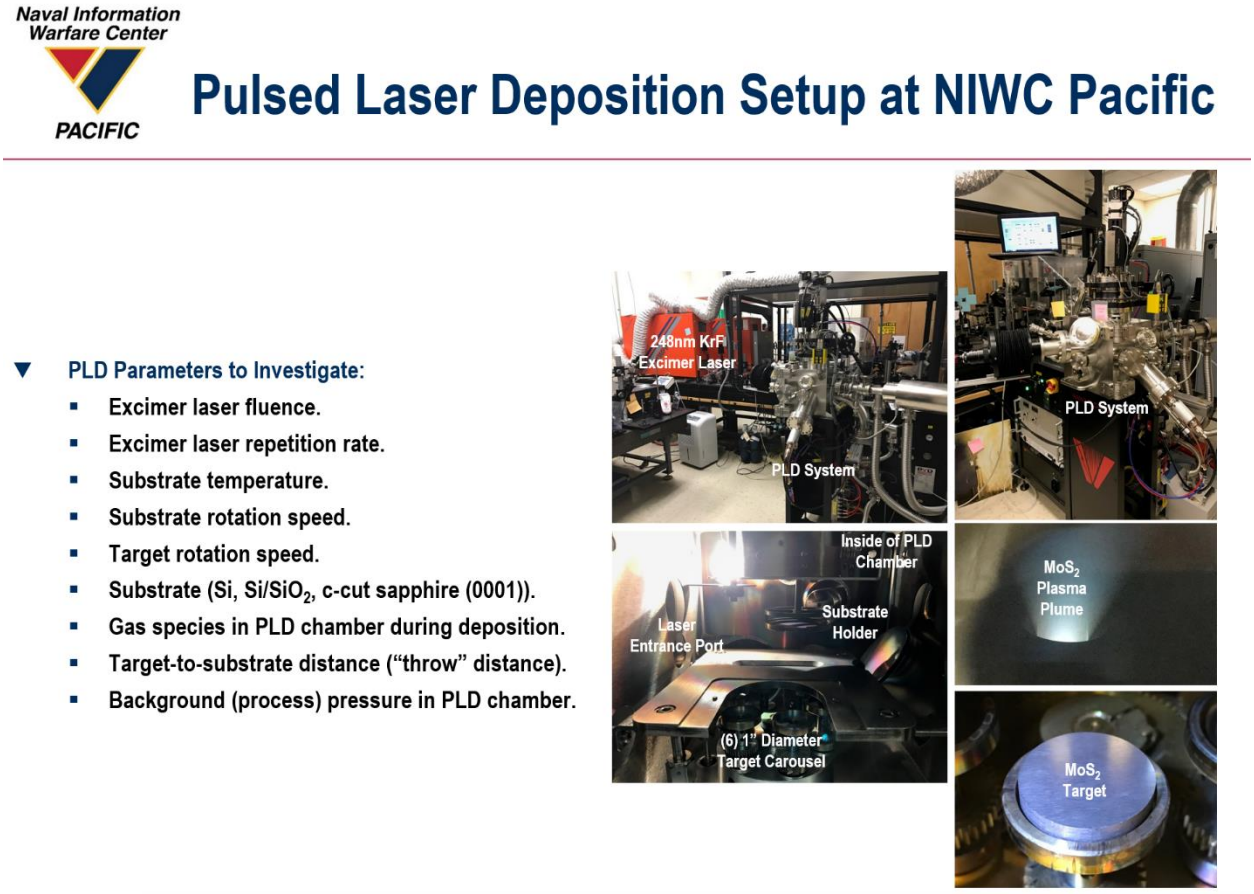

Figure 1. PLD setup at NIWC Pacific.

Figure 2 presents the PLD of 2D materials on sapphire (0001) substrates. (Top left) 20 PLD samples were shipped to our collaborators at the Naval Surface Warfare Center, Crane Division (NSWC Crane) for Fourier transform infrared (FTIR) spectroscopy measurements. (Bottom left) We diced 20 PLD 2-inch sapphire wafers into 9 ($1cm^2$) pieces to send to our collaborators (i.e., NSWC Crane, NIWC Pacific Hawaii for Raman spectroscopy, and the University of Oregon for x-ray diffraction (XRD).

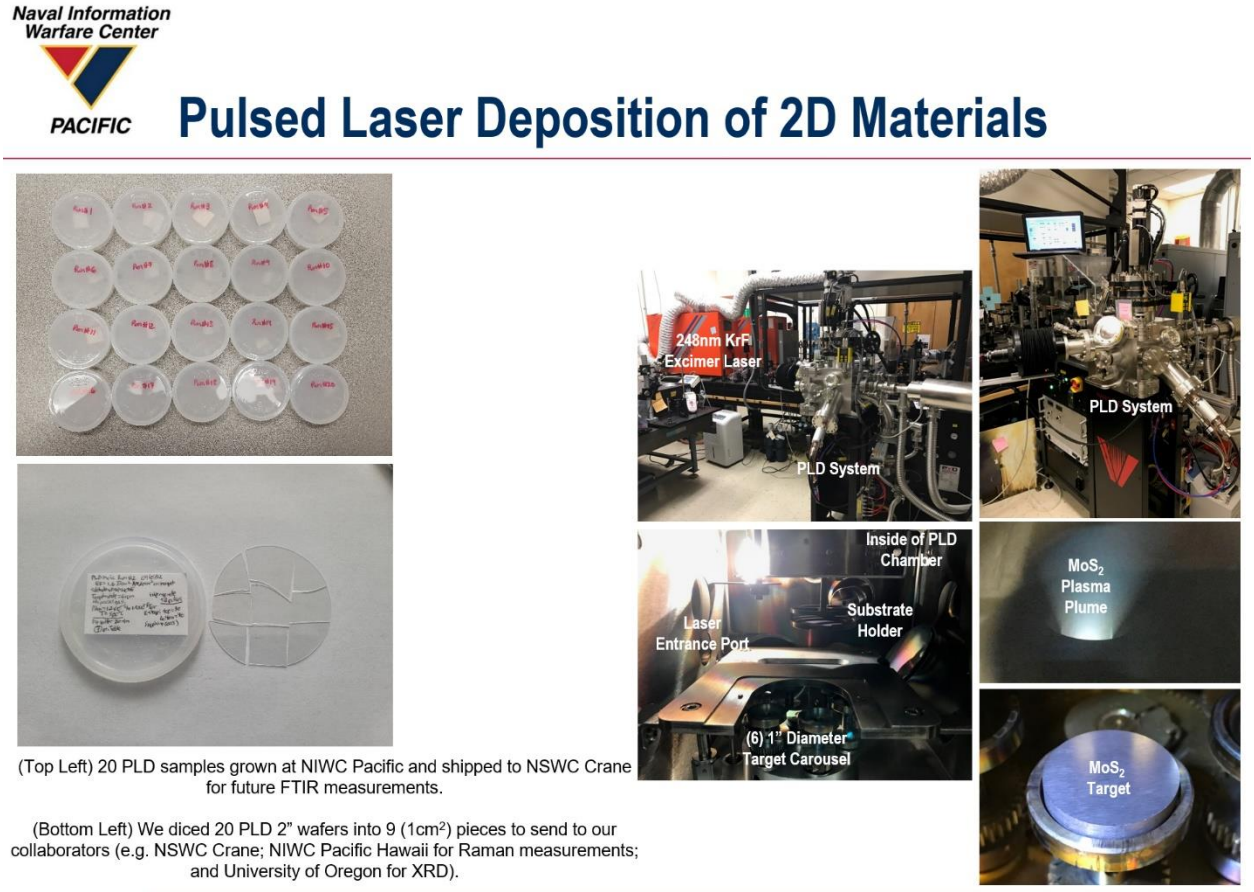

Figure 2. PLD of 2D materials.

Figure 3 displays PLD recipes for 20 experimental runs on 2-inch sapphire (0001) wafers. (Top panel) Recipes for depositing either molybdenum disulfide (MoS_2) or tungsten disulfide (WS_2) onto sapphire substrates. Refer to Table 1 and Table 2 for the same data. (Bottom panel) We diced 20 PLD 2-inch sapphire wafers into 9 ($1cm^2$) pieces to send to our collaborators (i.e., NSWC Crane for FTIR spectroscopy; NIWC Pacific Hawaii for Raman spectroscopy; and the University of Oregon for XRD).

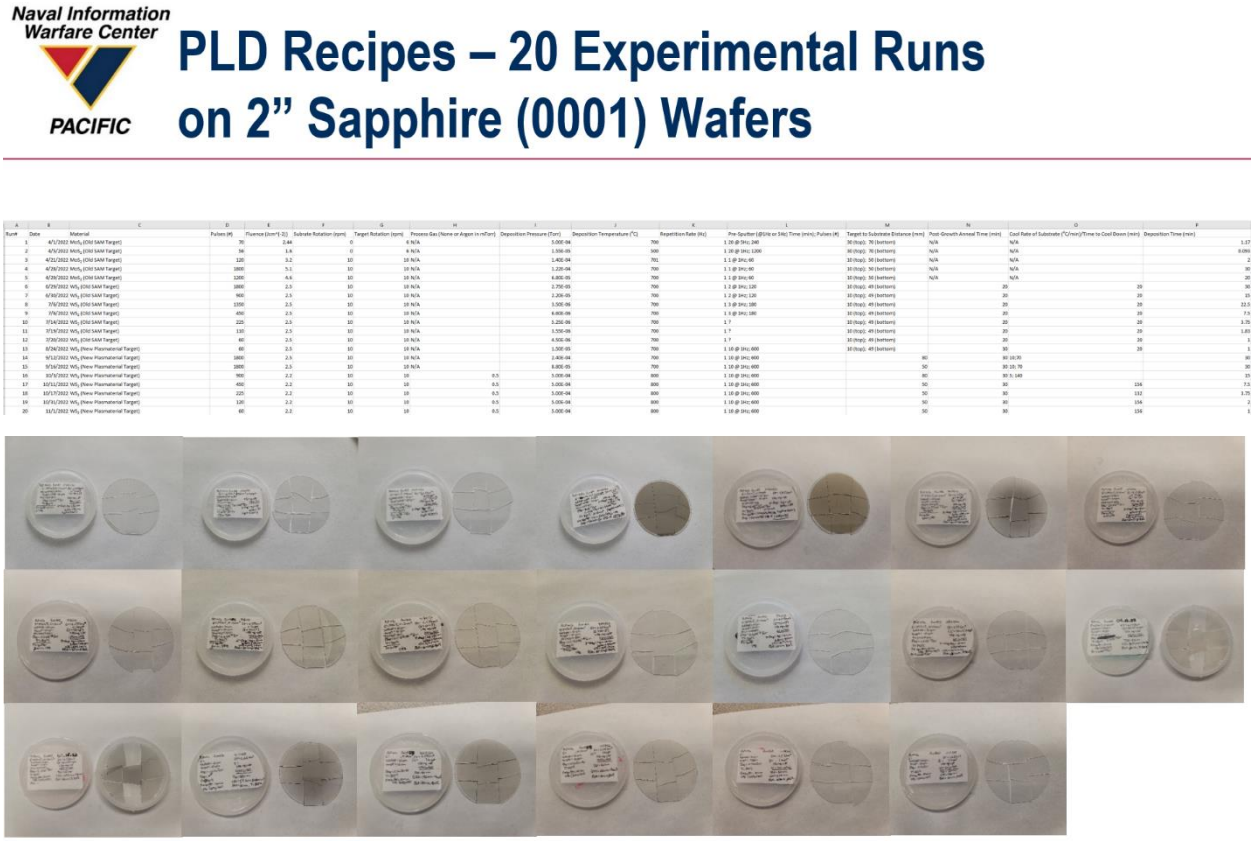

Figure 3. PLD recipes for 20 experimental runs on 2-inch sapphire (0001) wafers.

Table 1 shows the results for PLD experimental runs with associated parameters. The term Old SAM Target refers to ablation targets from Stanford Advanced Materials. Parameters include material, number of laser pulses, laser fluence, deposition pressure, deposition temperature, pre-sputter clean of the ablation targets, post-growth annealing of the substrate, target-to-substrate distance, and deposition time. The laser's repetition rate was 1 Hz.

Table 1. PLD experimental runs with associated parameters.

Run	Material	Pulses (#)	Fluence (Jcm^{-2})	Deposition Pressure (Torr)	Deposition Temperature (^oC)	Pre-Sputter (@1Hz or 5Hz) Time (min); Pulses (#)	Post-Growth Anneal Time (min)	Target to Substrate Distance (mm)	Deposition Time (min)
1	MoS_2 (Old SAM Target)	70	2.44	5e-4	700	5Hz; 20; 240	N/A	30 (top); 70 (bottom)	1.17
2	MoS_2 (Old SAM Target)	56	1.6	1.55e-5	500	1Hz; 20; 1200	N/A	30 (top); 70 (bottom)	0.093
3	MoS_2 (Old SAM Target)	120	3.2	1.4e-4	701	1Hz; 1; 60	N/A	10 (top); 50 (bottom)	2
4	MoS_2 (Old SAM Target)	1800	5.1	1.22e-4	700	1Hz; 1; 60	N/A	10 (top); 50 (bottom)	30
5	MoS_2 (Old SAM Target)	1200	4.6	6.8e-5	700	1Hz; 1; 60	N/A	10 (top); 50 (bottom)	20
6	WS_2 (Old SAM Target)	1800	2.5	2.75e-5	700	1Hz; 2; 120	20	10 (top); 49 (bottom)	30
7	WS_2 (Old SAM Target)	900	2.5	2.2e-5	700	1Hz; 2; 120	20	10 (top); 49 (bottom)	15
8	WS_2 (Old SAM Target)	1350	2.5	3.5e-6	700	1Hz; 3; 180	20	10 (top); 49 (bottom)	22.5
9	WS_2 (Old SAM Target)	450	2.5	6.6e-6	700	1Hz; 3; 180	20	10 (top); 49 (bottom)	7.5
10	WS_2 (Old SAM Target)	225	2.5	5.25e-6	700	?	20	10 (top); 49 (bottom)	3.75

Table 2 presents a continuation of PLD experimental runs with associated parameters. New Plasmaterial Target refers to an ablation target from Plasmaterials, Inc. Parameters include material, number of laser pulses, laser fluence, deposition pressure, deposition temperature, pre-sputter clean of the ablation targets, post-growth anneal of the substrate, target-to-substrate distance, and deposition time. The laser's repetition rate was 1 Hz.

Table 2. Continuation of PLD experimental runs with associated parameters.

Run	Material	Pulses (#)	Fluence (Jcm^{-2})	Deposition Pressure (Torr)	Deposition Temperature (°C)	Pre-Sputter (@1Hz or 5Hz) Time (min); Pulses (#)	Post-Growth Anneal Time (min)	Target to Substrate Distance (mm)	Deposition Time (min)
11	WS_2 (Old SAM Target)	110	2.5	3.55e-6	700	?	20	10 (top); 49 (bottom)	1.83
12	WS_2 (Old SAM Target)	60	2.5	4.5e-6	700	?	20	10 (top); 49 (bottom)	1
13	WS_2 (New Plasmaterial Target)	60	2.5	1.5e-5	700	1Hz; 10; 600	30	10 (top); 49 (bottom)	1
14	WS_2 (New Plasmaterial Target)	1800	2.5	2.4e-4	700	1Hz; 10; 600	30	80	30
15	WS_2 (New Plasmaterial Target)	1800	2.5	8.8e-5	700	1Hz; 10; 600	30	50	30
16	WS_2 (New Plasmaterial Target)	900	2.2	5e-4	800	1Hz; 10; 600	30	80	15
17	WS_2 (New Plasmaterial Target)	450	2.2	5e-4	800	1Hz; 10; 600	30	50	7.5
18	WS_2 (New Plasmaterial Target)	225	2.2	5e-4	800	1Hz; 10; 600	30	50	3.75
19	WS_2 (New Plasmaterial Target)	120	2.2	5e-4	800	1Hz; 10; 600	30	50	2
20	WS_2 (New Plasmaterial Target)	60	2.2	5e-4	800	1Hz; 10; 600	30	50	1

We sent the PLD MoS_2 and PLD WS_2 samples on sapphire substrates to the University of Oregon for x-ray diffraction (XRD) and x-ray reflectivity (XRR) measurements. Figure 4 displays (top left) grazing incidence XRD of 3 PLD recipe/run samples. (Top right) Specular XRD of 5 PLD recipe/run samples. (Bottom left) XRR of 8 PLD recipe/run samples. The samples are too thin (from XRR) to calculate their thicknesses. (Bottom right) XRR (zoomed in from 0 to 1 degree) of 8 PLD recipe/run samples. We see XRD peaks for run 9, 10, and 12. This indicates that our PLD deposition rate is much lower than expected, thus we will grow samples with much more laser pulses than previously.

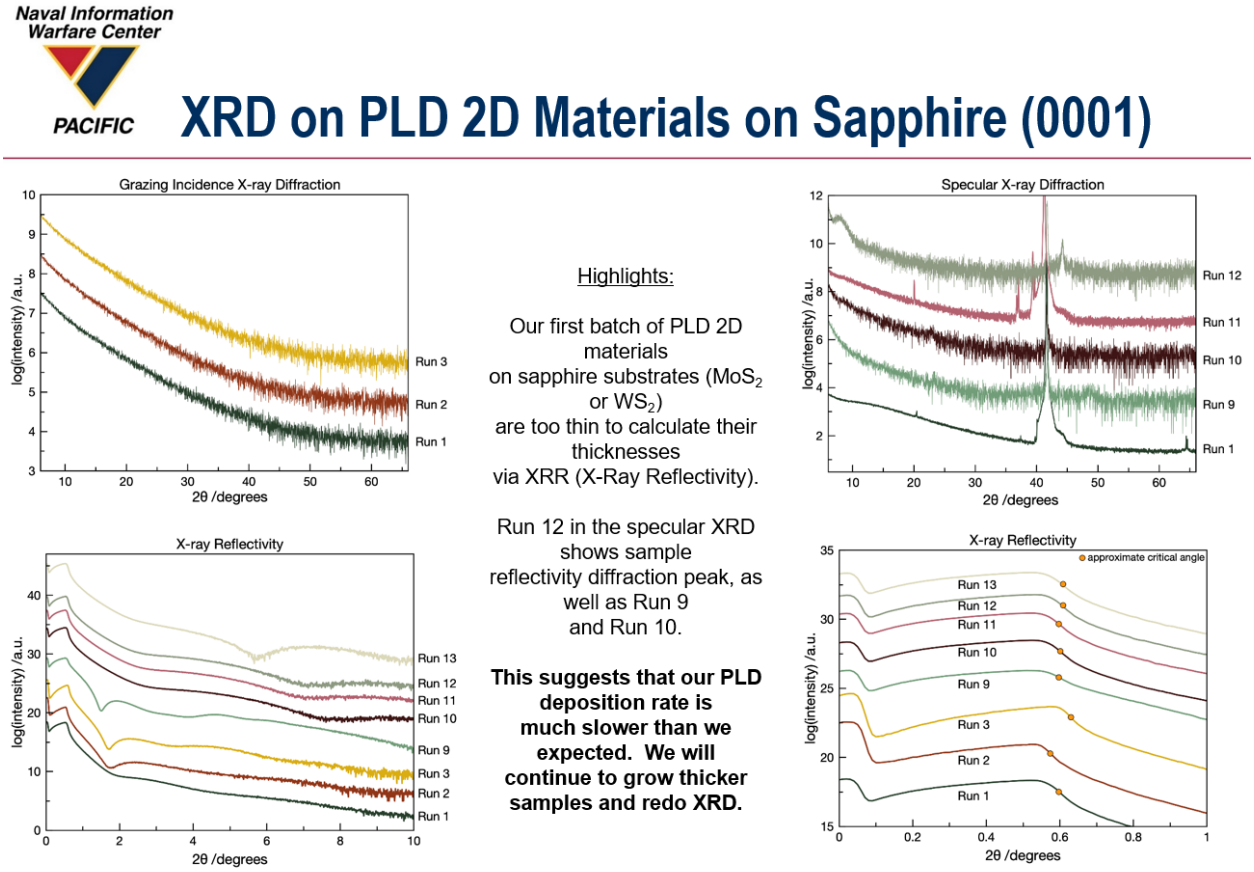

Figure 4. XRD on PLD 2D materials on sapphire (0001).

Figure 5 introduces (top left) specular XRD of 4 PLD recipe/run samples. (Bottom left) XRR (zoomed in from 0.2 to 0.8 degrees) of 4 PLD recipe/run samples. (Right) XRR of 4 PLD recipe/run samples. We see XRD peaks for runs 14, 15, 16, and 17. We now have a lock on which PLD recipes to focus on (i.e., runs 14 and 15). We will vary PLD parameters to grow more samples and subsequently send the new samples for XRD.

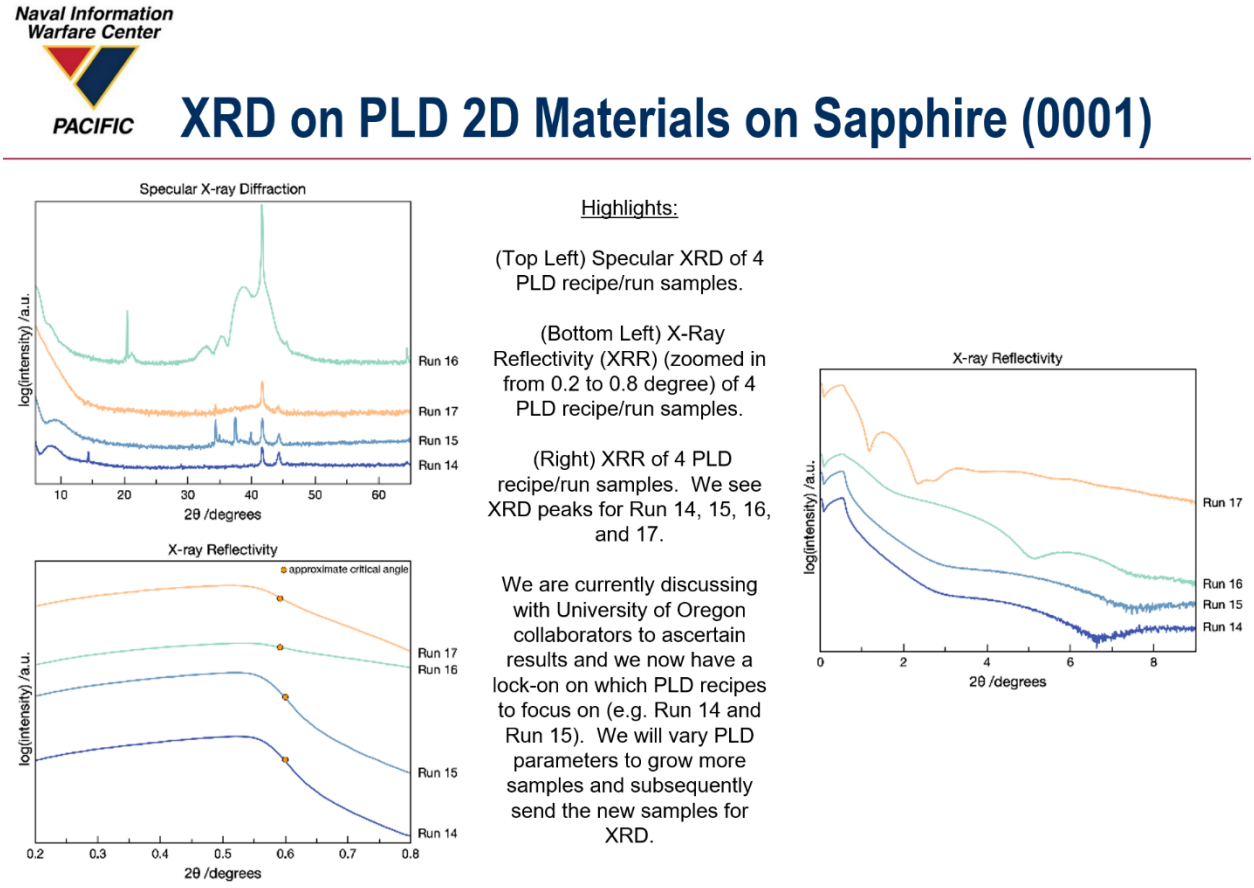

Figure 5. XRD on PLD 2D materials on sapphire (0001).

Figure 6 displays FTIR spectroscopy on PLD WS_2 on sapphire (0001) substrates sent to NSWC Crane. It seems that we start depositing PLD WS_2 material onto sapphire (0001) substrate (thickness currently unknown) starting from 450 pulses onward. This means that our deposition rate is much slower than that listed in the literature (typically 60 pulses per monolayer). This FTIR data, taken by our collaborators at NSWC Crane, corroborates the XRD data from the previous slides in that our material deposition commences at over 450 pulses.

Naval Information Warfare Center PACIFIC

FTIR Spectroscopy on PLD WS_2 on Sapphire

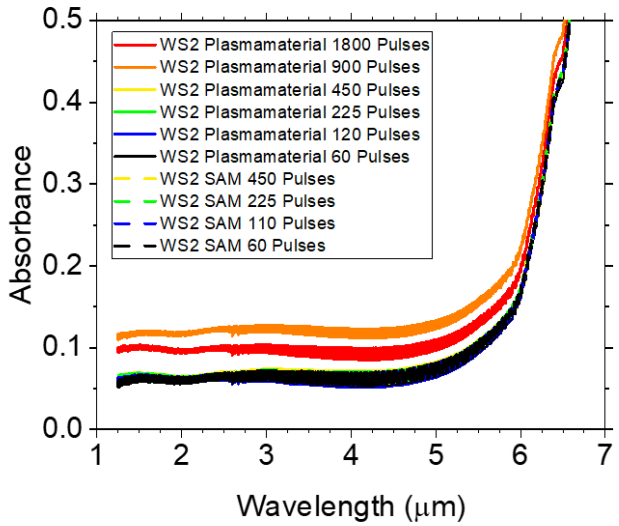

Highlights:

It seems that we start depositing PLD WS_2 material onto sapphire (0001) substrate (thickness currently unknown) starting from 450 pulses onward. This means that our deposition rate is much slower than that listed in the literature (typically 60 pulses per monolayer).

This FTIR data, taken by our collaborators at NSWC Crane (Indiana) corroborates the XRD data from the previous slides in that **our material deposition commences at over 450 pulses.**

Figure 6. FTIR spectroscopy on PLD WS_2 on sapphire.

In FY22 (Figure 7), we focused on establishing a novel in-house NIWC Pacific capability of cryogenic PL spectroscopy setup using bare multi-mode fibers (MMF) as local probes that are sensitive enough to detect weak PL signals from monolayer 2D semiconductors on sapphire substrates. It's important to note that this novel experimental setup does not use objective lenses and thus enables facile and rapid local electrical and optical probing of active 2D materials and devices for research, development, test, and evaluation (RDT&E) purposes from base temperature (i.e., 5K) to elevated temperatures (i.e., 500K). (Left) An experimental custom setup in the QENDL lab shows the various equipment used: a 532nm diode-pumped solid-state laser (DPSSL), fiber coupled from a single mode fiber (SMF) into an input fiber bench featuring a 532nm laser clean-up filter and a 550nm short-pass filter to ensure that only 532nm photoexcites the sample (i.e., eliminate any other contributions from the DPSSL), and then fiber coupled into a MMF that is vacuum feedthrough connected into the vacuum chamber.

Inside the probe station vacuum chamber, MMF is stripped bare and rests at a 30° angle on a custom 3D-printed fiber optic holder mounted onto an XYZ micro-manipulator probe arm that serves as the photoexcitation arm. A similar setup implemented for the photodetection fiber optic probe arm serves to locally probe the scattered light from the monolayer 2D semiconductor on a sapphire substrate resting on a sample mount in the vicinity of the photoexcitation laser region. This scattered light is routed outside of the probe station vacuum chamber and into an output fiber bench that features various long-pass filters, and then routed into an Ocean Optics QE Pro modular spectrometer. (Right panels) Various images of the monolayer 2D semiconductors on sapphire (0001) substrates being photoexcited via fiber optic probe arms at 532nm; an image of 4 electrical probe arms and 2 fiber optic probe arms with 2D material-based devices on a sample mount, etc.

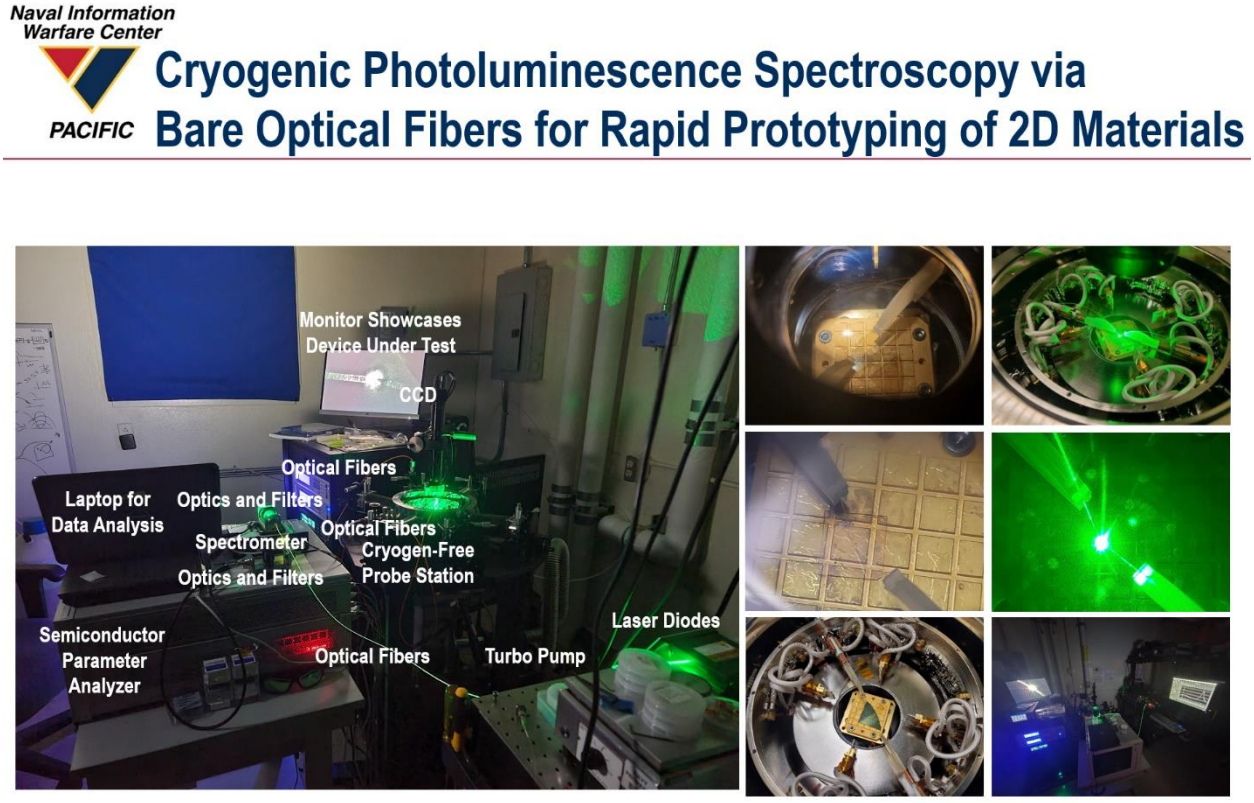

Figure 7. Cryogenic PL spectroscopy via bare optical fibers for rapid prototyping of 2D materials.

Figure 8 presents the PL of commercial off-the-shelf (COTS) 2D semiconductors on sapphire (0001) substrates using our Lake Shore CRX-VF cryogen-free probe station. (Left) We demonstrate that our novel setup has the sensitivity to detect PL signals from large-area CVD monolayer 2D semiconductors on sapphire substrates at room temperature. We observe direct bandgap (i.e., A exciton) luminescence from three separate transition metal dichalcogenides (TMDs) (i.e., MoS_2, WSe_2, and WS_2) using only bare MMF and no objective lenses. (Right) 2 fiber optic probe arms with bare MMF resting at about 30° angle incidence on a custom 3D printed fiber holder to locally photoexcite and photodetect PL signals from 2D semiconductors, in view of an experimental setup during a measurement.

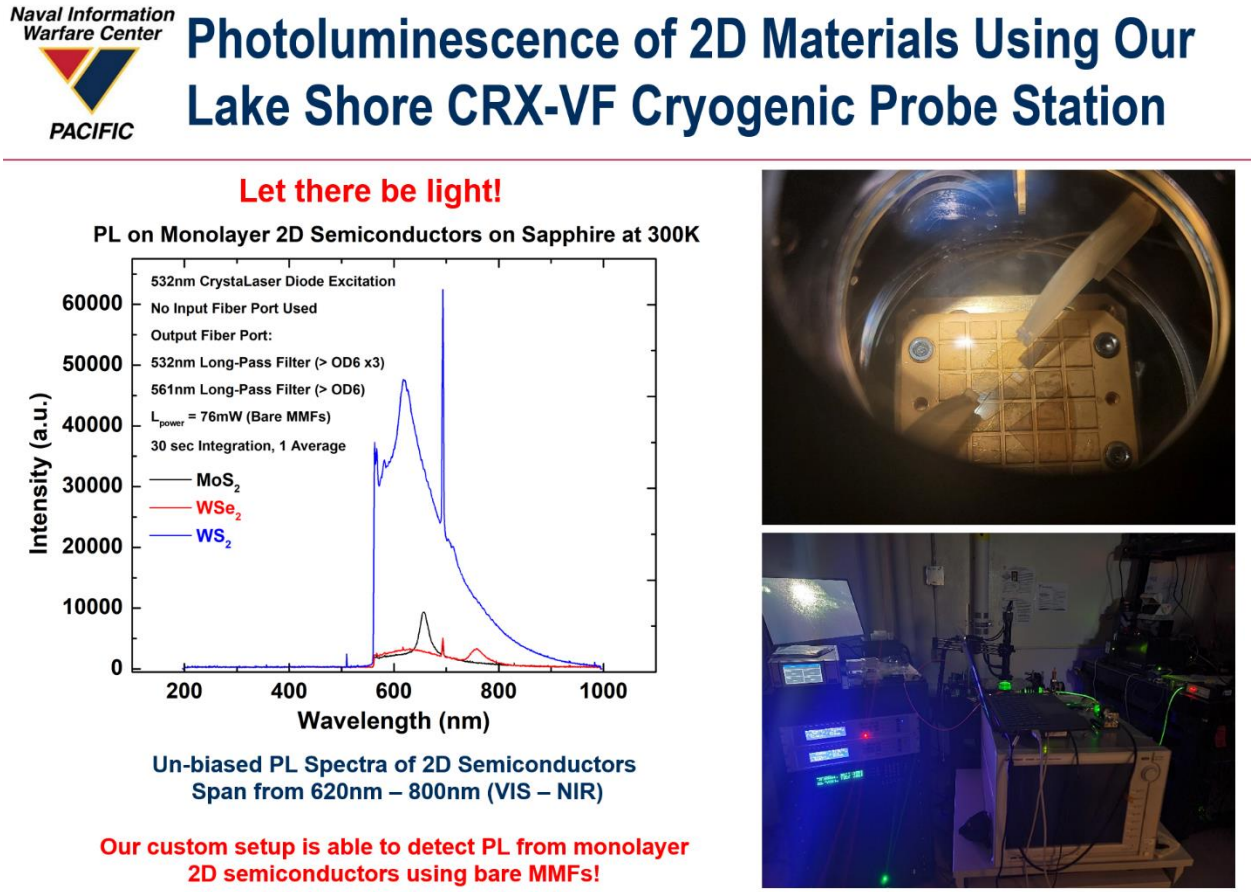

Figure 8. PL of 2D materials using our Lake Shore CRX-VF cryogen-free probe station.

Figure 9 indicates the cryogenic PL spectroscopy measurement setup at Battery Ashburn Laboratory in NIWC Pacific in FY23. Back in February 2023, we noticed that our 10kW chiller in the QENDL lab was having a heat load issue with cooling down our cryogenic probe station (i.e., it could not cool down the Helium compressor for more than 15 minutes after turning the compressor on). We decided to take apart the fiber optic probe arm assembly and re-setup the cryogenic PL setup using the Lake Shore CRX-4K cryogenic probe station in Battery Ashburn. This attempt was successful and was completed in about one and a half days. (Top left to top right images) MMF vacuum feedthrough is sealed with epoxy, and MMF serves as the photodetection probe arm that detects the scattered light from our sample. A single-mode fiber (SMF) vacuum feedthrough is sealed with epoxy and serves as the photoexcitation probe arm to excite our sample using a 532nm continuous-wave laser diode.

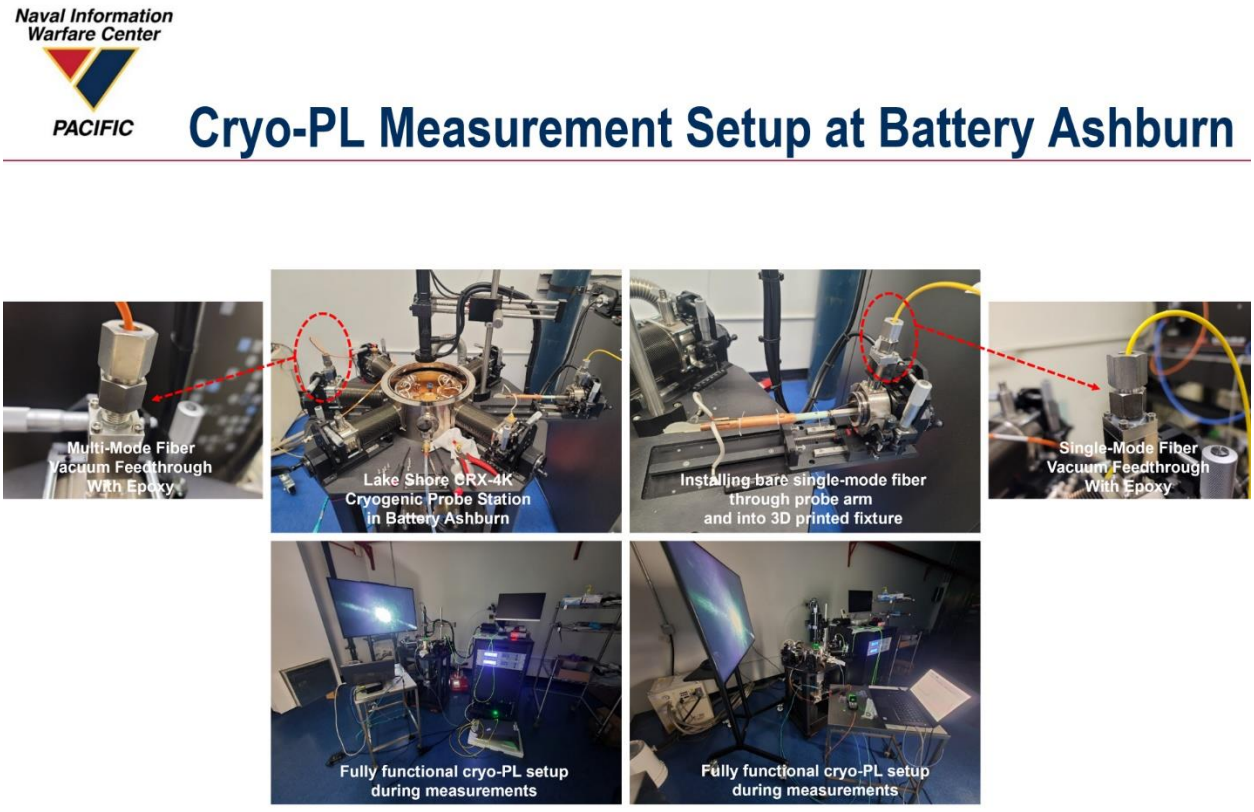

Figure 9. Cryo-PL measurement setup at Battery Ashburn.

Figure 10 demonstrates the lens-less cryogenic PL spectroscopy setup for rapid prototyping of 2D quantum heterostructures. This setup allows us to rapidly probe the active region of our samples or devices using up to four direct current (DC) electrical probe arms and two fiber optic probe arms. Please refer to the listed publication [7] on the slide for further details.

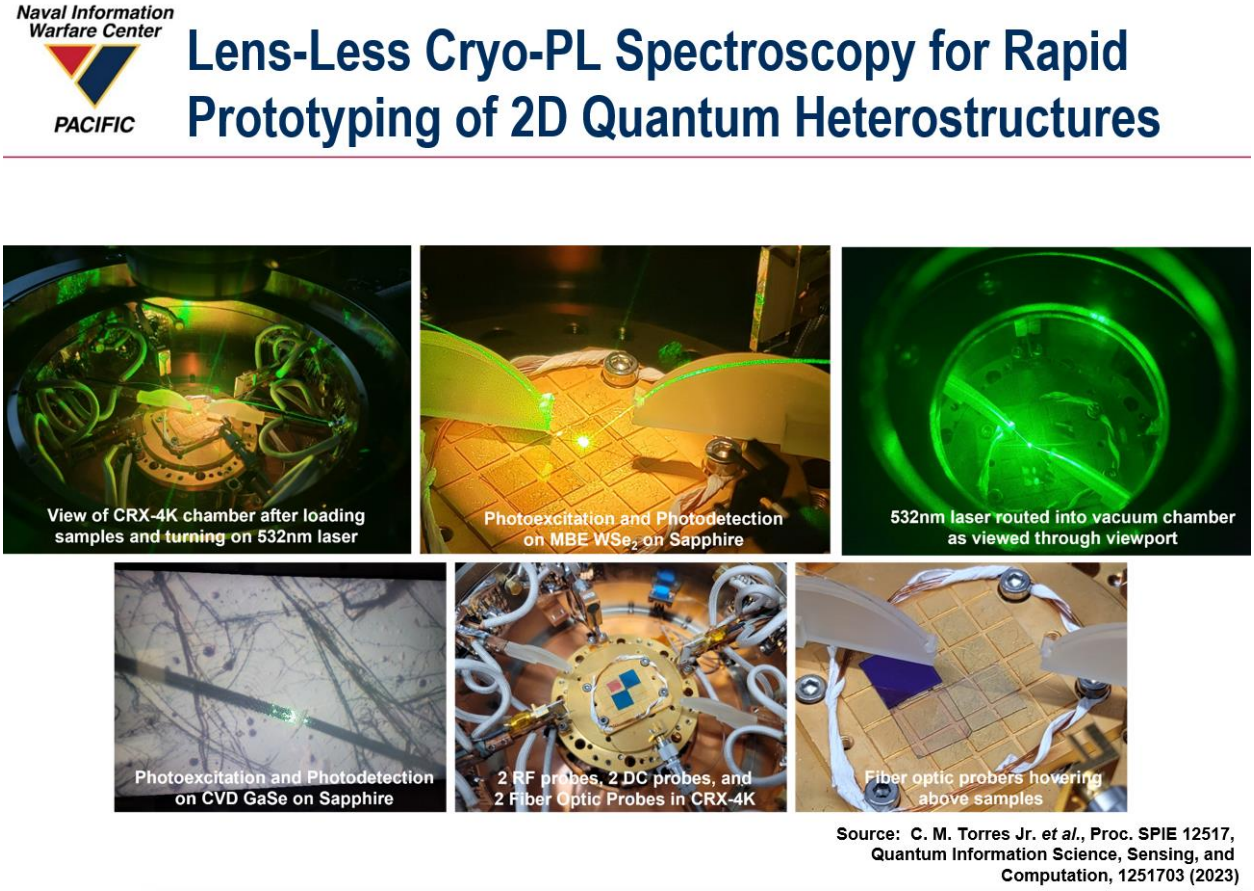

Figure 10. Lens-less cryo-PL spectroscopy for rapid prototyping of 2D quantum heterostructures.

The cryogenic PL spectroscopy of COTS CVD WS_2 on a sapphire (0001) substrate is shown in Figure 11. (Left) Temperature dependence of PL of monolayer WS_2 on sapphire (0001) substrate (semi-log scale). We observe a red shift of the direct bandgap (i.e., A exciton) luminescence from monolayer WS_2 of about 40nm when changing the temperature from 8.5K to 450K. The experimental parameters applied to the measurement are listed in the legend. (Center) The same data as before, but full-spectrum (linear scale) instead of the zoomed-in spectrum (semi-log scale) near the direct bandgap region of monolayer WS_2. The sharp peaks near 693nm are an artifact from the laser spectrum and do not derive from the 2D semiconductor. (Right) 532nm laser diode coupled into the cryogenic chamber with the chamber lids open to show all six probe arms. Please refer to the listed publication [6] on the slide for further details.

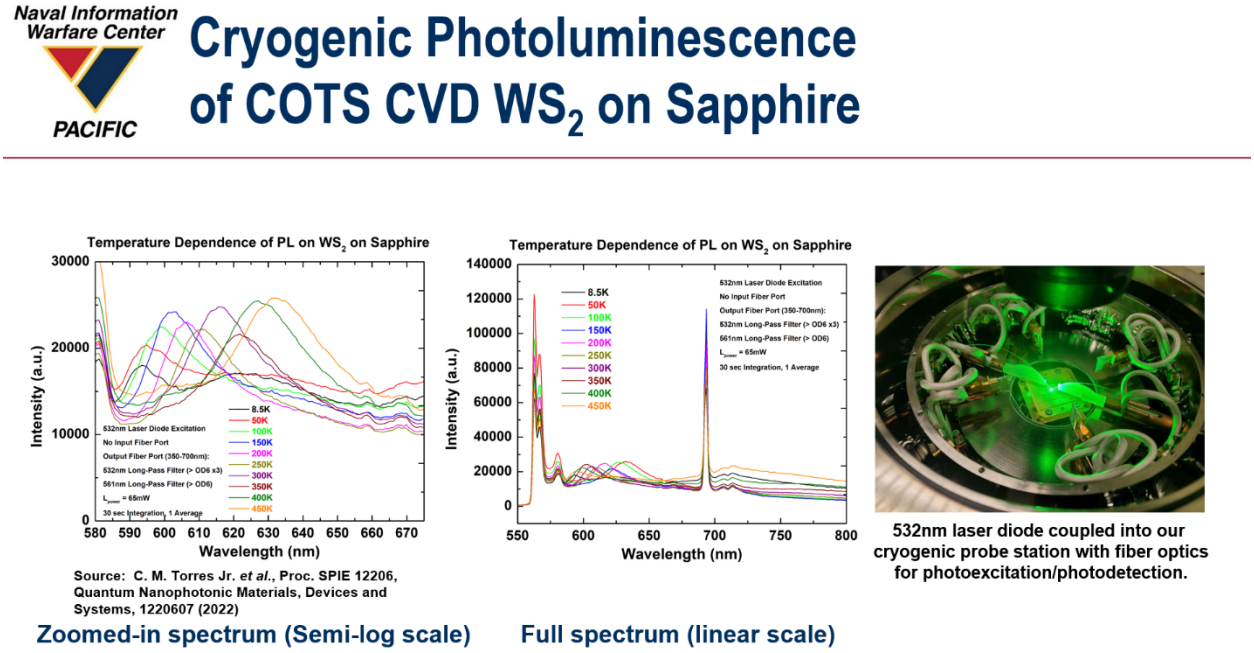

Figure 11. Cryogenic PL of COTS CVD WS_2 on sapphire.

The picture in Figure 12 shows cryogenic PL spectroscopy of COTS Molecular Beam Epitaxy (MBE) Molybdenum Diselenide ($MoSe_2$) on a sapphire (0001) substrate. (Left) Temperature dependence of PL of monolayer $MoSe_2$ on sapphire (0001) substrate (semi-log scale) for sample 1. We observe a red shift of the direct bandgap (i.e., A exciton) luminescence from monolayer $MoSe_2$ of about 37nm when changing the temperature from 6K to 450K. The experimental parameters used in the measurement are listed in the legend. (Center) The same data as before, but on a linear scale. (Right) Temperature dependence of PL of monolayer $MoSe_2$ on sapphire (0001) substrate (linear scale) for sample 2 from 10K to 180K corroborates the results from sample 1. Please refer to the listed publication [6] on the slide for further details.

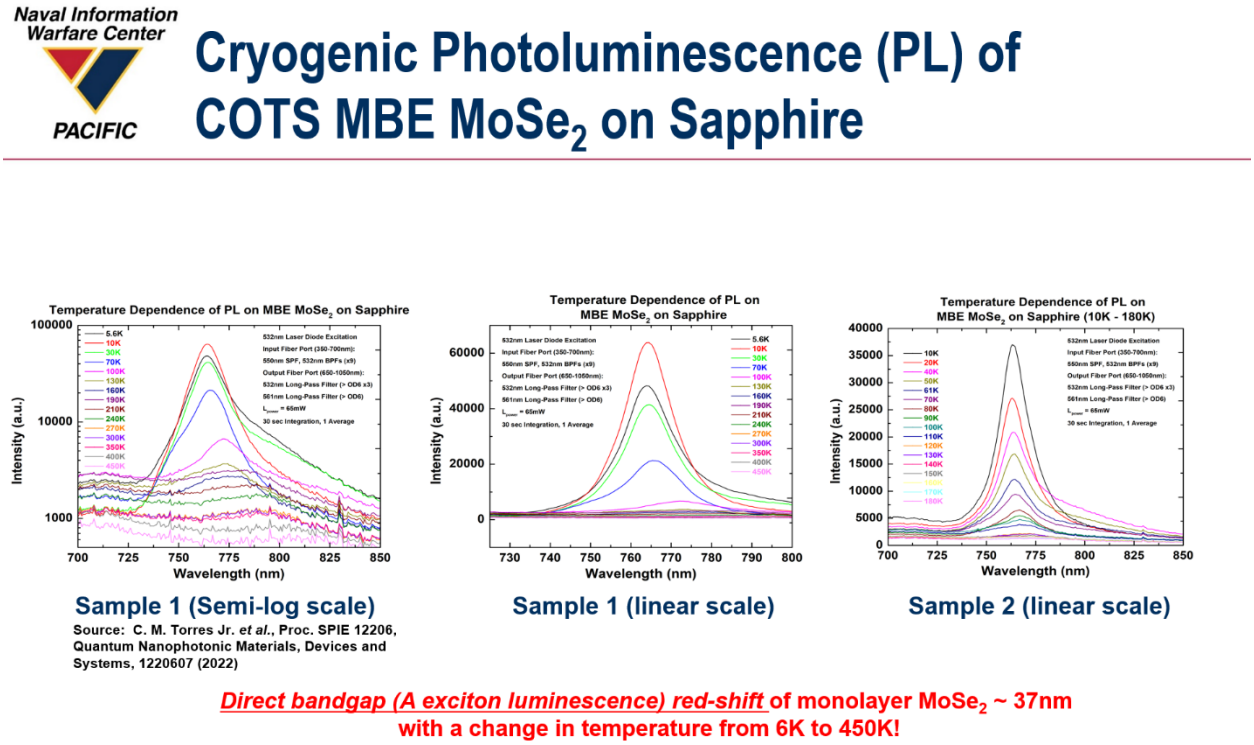

Figure 12. Cryogenic PL of COTS MBE $MoSe_2$ on sapphire.

Figure 13 shows a direct bandgap modulation with increasing temperature of COTS large-area CVD WSe_2 on sapphire (0001) substrate. Using this novel setup, we observe a PL peak wavelength shift (i.e., direct bandgap shift) of about 41nm when the temperature of CVD WSe_2 on sapphire (0001) substrate is raised from around 9K to 450K. We fit the data to the equation shown, which describes the temperature dependence of semiconductor bandgaps using a Python script, and it resulted in 19meV for the average phonon energy for CVD monolayer WSe_2 on sapphire (0001) substrate. Please refer to the listed publications [6, 7] on the slide for further details.

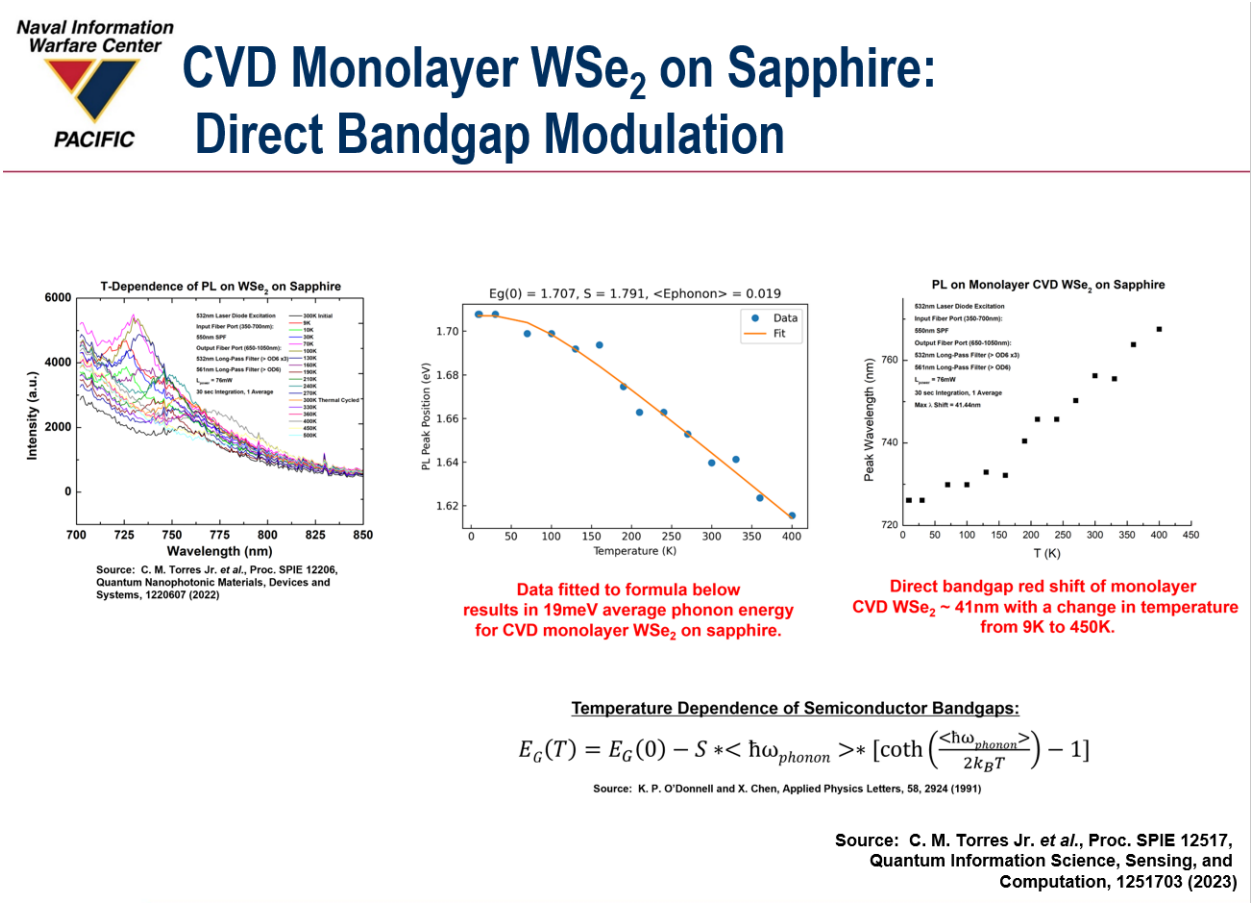

Figure 13. Direct bandgap modulation of CVD monolayer WSe_2 on sapphire.

Figure 14 corroborates a direct bandgap modulation with increasing temperature and the extraction of exciton binding energy of COTS large-area MBE WSe_2 on sapphire (0001) substrate. Using this novel setup, we observe a PL peak wavelength shift (i.e., direct bandgap shift) of about 32nm when the temperature of MBE WSe_2 on sapphire (0001) substrate is raised from around 3.7K to 350K. We fit the data to the equation shown in Figure 13, which describes the temperature dependence of semiconductor bandgaps using a Python script, and it resulted in 41meV for the average phonon energy for MBE monolayer WSe_2 on sapphire (0001) substrate. We also fit the data to the Arrhenius equation shown in Figure 14 to extract an exciton binding energy of 92meV for MBE WSe_2 on a sapphire (0001) substrate. Please refer to the listed publication [7] on the slide for further details.

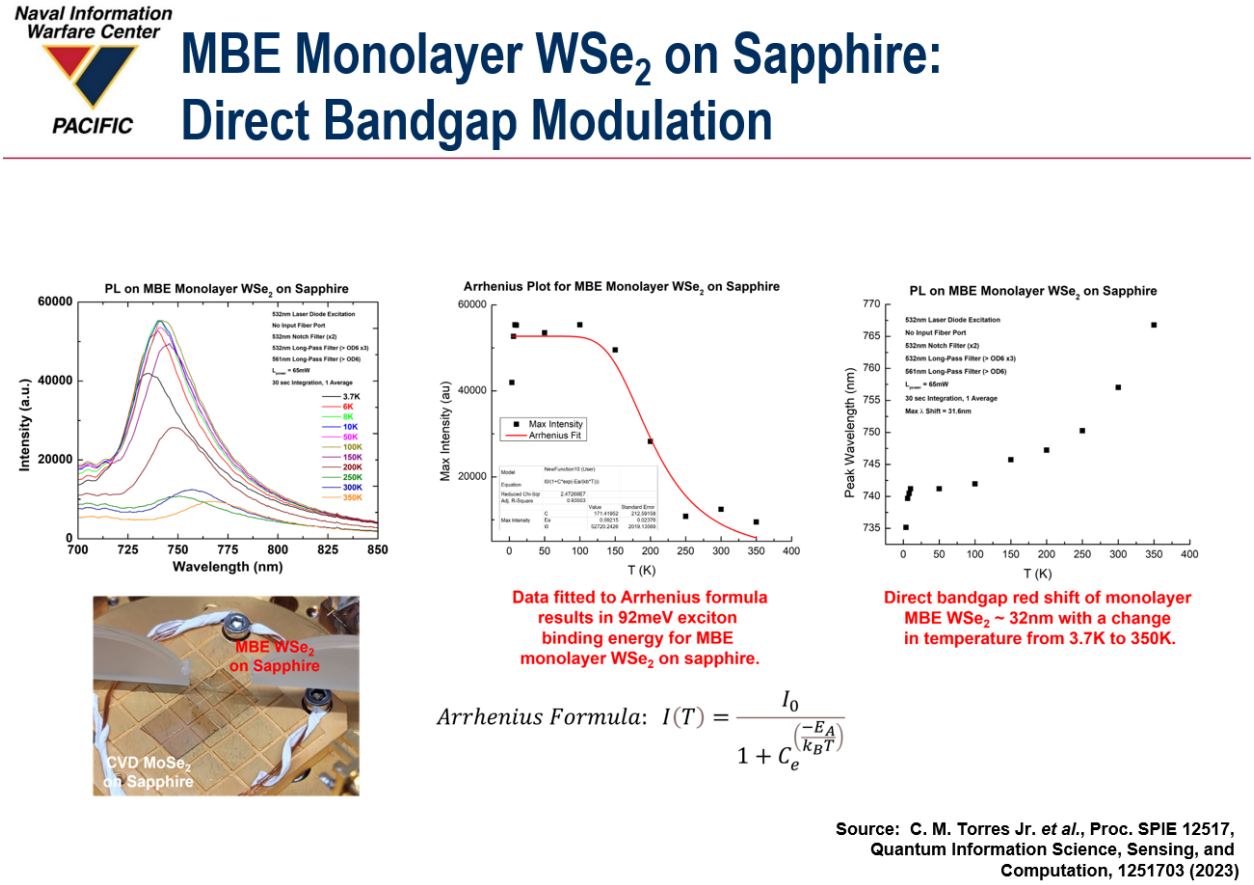

Figure 14. Direct bandgap modulation of MBE WSe_2 on sapphire.

Figure 15 shows cryogenic PL spectroscopy of COTS CVD monolayer MoS_2 on sapphire (0001) substrates. (Left) Temperature dependence of PL on CVD monolayer MoS_2 on sapphire (0001) substrate for a sample at 300K (red curve) and 7K (black curve). At 300K, we observe the sharp full width at half maximum (FWHM of about 25nm) A free exciton (i.e., direct bandgap) luminescence signal. Upon cool down to 7K, the A free exciton PL signal decreases in intensity and blue shifts, whereas an intense and broad defect PL spectrum centered near 710nm and attributed to bound excitons in monolayer MoS_2 dominates. Experimental parameters are listed in the legend. (Center) Temperature dependence of PL on CVD monolayer MoS_2 on sapphire (0001) substrate for another sample after thermal cycling from 300K (initial) to 5.35K and back to 300K (final). Experimental parameters are listed in the legend. (Right) Temperature dependence of PL on CVD monolayer MoS_2 on sapphire (0001) substrate for another sample from 5.35K to 190K. This graph clearly shows the co-existence and evolution of both the A exciton (i.e., direct bandgap) PL signal and the bound exciton defect PL signal from 5.35K to 190K. The bound exciton PL spectrum dominates the A exciton signal for temperatures up to about 100K. The bound exciton PL spectrum red shifts with increasing temperature up to about 100K, beyond which it disappears. The A exciton PL spectrum also red shifts with increasing temperature but features a lower intensity than the bound exciton defect PL signal for temperatures below 100K. Please refer to the listed publications [6, 7] on the slide for further details.

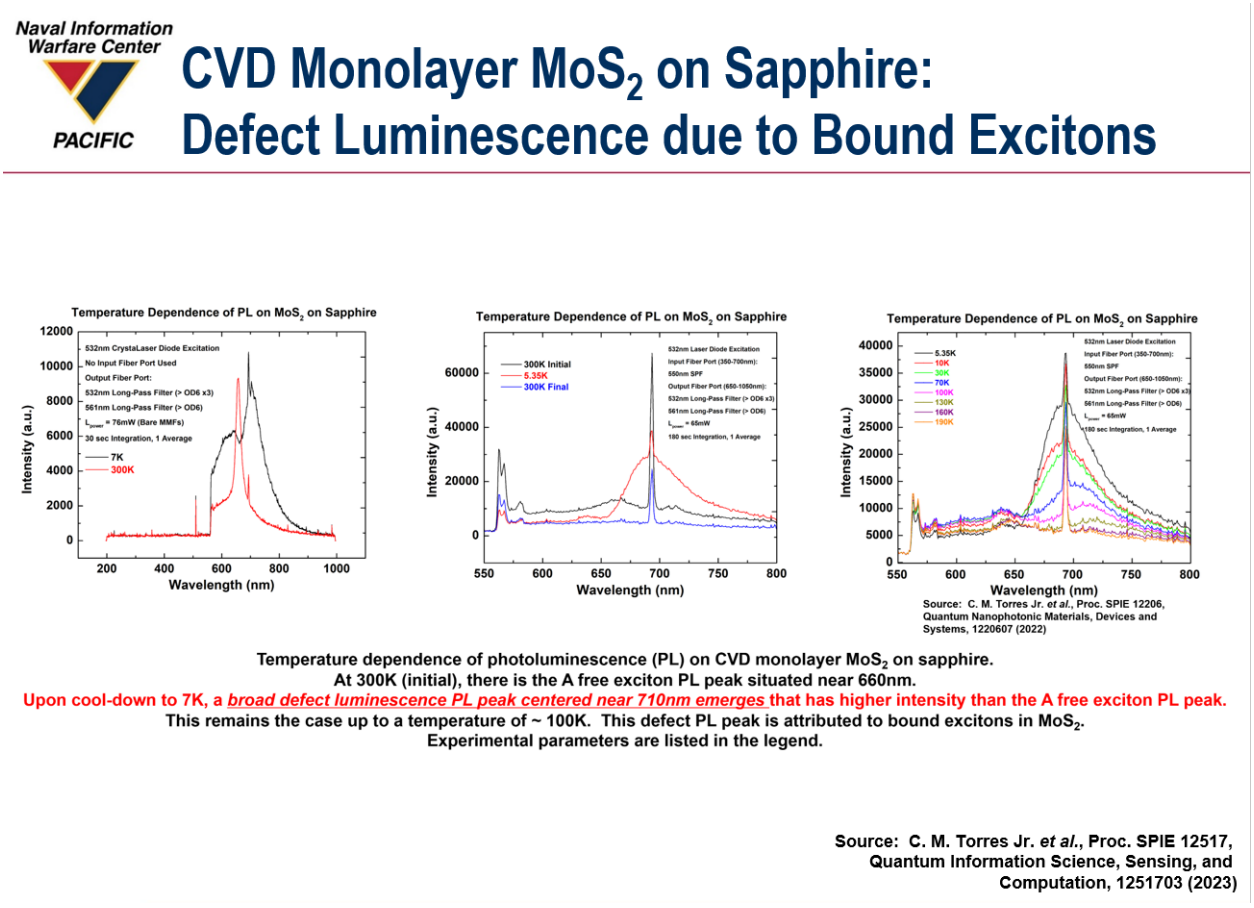

Figure 15. Defect luminescence due to bound excitons in CVD monolayer MoS_2 on sapphire.

Figure 16 presents a summary of the material characterization using our novel fiber-optic-based cryogenic PL spectroscopy setup in the QENDL lab at NIWC Pacific. The various materials studied are listed in the far-left column, with their corresponding substrates listed in the next column. The following three columns list the PL peak wavelength shift in nm (PL peak direct bandgap energy shift in meV), the extracted average phonon energies from the fitted data using a Python script, the equation for temperature dependence of the semiconductor bandgap (shown in Figure 13), and the corresponding temperature range of the measured samples. Please refer to the listed publication [7] on the slide for further details.

Naval Information Warfare Center PACIFIC

Summary of Material Characterization

Material	Substrate	$\Delta\lambda$ (ΔE)	$\langle\hbar\omega_{phonon}\rangle$	Temperature
CVD WSe_2	Sapphire (0001)	41nm (30.2meV)	19meV	9K-450K
MBE WSe_2	Sapphire (0001)	32nm (38.8meV	41meV	3.7K-350K
CVD WS_2	Sapphire (0001)	38nm (32.6meV	11meV	8.5K-450K
MBE WS_2	Sapphire (0001)	25nm (49.6meV)	37meV	3.7K-350K
CVD $MoSe_2$	Sapphire (0001)	37nm (33.5meV)	32meV	3.7K-350K
MBE $MoSe_2$	Sapphire (0001)	30nm (41.3meV)	53meV	3.7-360K
CVD MoS_2-CVD 1L hBN	SiO_2/Silicon	8nm (variability)	53meV	3.7K-350K
CVD WS_2-CVD 1L hBN	Sapphire (0001)	7nm (variability)	129meV	3.7K-350K
CVD WSe_2-$MoSe_2$	Sapphire (0001)	39nm (31.8meV)	15meV	3.7K-350K

Source: C. M. Torres Jr. *et al.*, Proc. SPIE 12517, Quantum Information Science, Sensing, and Computation, 1251703 (2023)

Figure 16. Summary of the material characterization.

3. CONCLUSIONS

This technical report summarized the work executed during FY21–FY23 of the ONR-funded Electrically-Tunable On-Demand Energy Bandstructures in Pulse Laser Deposited 2D Quantum Material Heterostructure-Based Devices (Qu-PLD) project and during FY21–FY22 of the NIWC Pacific NISE-funded Quantum Engineered Nanodevices Exploiting Twistronics for EMW and C4ISR project. Most of the work was performed by NIWC Pacific scientists and engineers in the QENDL at NIWC Pacific in San Diego, CA.

This page is intentionally blank.

REFERENCES

[1] Department of the Navy 30 Year RDT+E 30 Year Research and Development Plan (2017); https://blog.spawar.navy.mil/command/DON%2030%20Year%20R%26D%20Plan%20FINAL_5Jan2017C.PDF

[2] ONR Naval Science and Technology (S+T) Strategy (2015); http://www.defenseinnovationmarketplace.mil/resources/NavalS&TStrategy2015_Final_01-26-15.pdf

[3] National Defense Science and Technology Strategy (2023); https://media.defense.gov/2023/May/09/2003218877/-1/-1/0/NDSTS-FINAL-WEB-VERSION.PDF

[4] C. M. Torres Jr., "Establishing the Quantum Engineered Nano Devices Laboratory (QENDL) at NIWC Pacific," Defense Technical Information Center (DTIC), Technical Report, Accession Number AD1120262, (2021).

[5] C. M. Torres Jr. et al., "Towards Voltage-Tunable Wavelength Agile 2D Material-Based Light-Emitting Transistors (2D-LETs)", Proceedings of the SPIE, Nanoscale and Quantum Materials: From Synthesis and Laser Processing to Applications 2022, 11990, 1199003, 1-23 (2022).

[6] C. M. Torres Jr. et al., "Cryogenic Photoluminescence Setup for Rapid Prototyping and Active Device Biasing of Monolayer 2D Semiconductors for Quantum Applications," Proceedings of the SPIE, Quantum Nanophotonic Materials, Devices, and Systems 2022, 12206, 1220607, 1–12 (2022).

[7] C. M. Torres Jr. et al., "A Rapid Prototyping Approach Towards Cryogenic Photoluminescence Spectroscopy of Monolayer Transition Metal Dichalcogenides and Their Heterostructures," Proceedings of the SPIE, Quantum Information Science, Sensing, and Computation 2023, 12517, 1251703, 9–28 (2023).

This page is intentionally blank.

INITIAL DISTRIBUTION

84310	Technical Library/Archives	(1)
55360	C. Torres Jr.	(1)
55360	A. Hening	(1)
55360	M. Pascoguin	(1)
55360	J. Adleman	(1)

Defense Technical Information Center
Fort Belvoir, VA 22060–6218 (1)

Office of Naval Research (1)
Naval Innovative Science and Engineering (1)

This page is intentionally blank.

REPORT DOCUMENTATION PAGE

Form Approved
OMB No. 0704-01-0188

PLEASE DO NOT RETURN YOUR FORM TO THE ABOVE ADDRESS.

1. REPORT DATE *(DD-MM-YYYY)*	2. REPORT TYPE	3. DATES COVERED *(From - To)*
February 2024	Final	

4. TITLE AND SUBTITLE

Towards Pulsed Laser Deposition of 2D Materials and Cryogenic Photoluminescence Spectroscopy of 2D Transition Metal Dichalcogenides

5a. CONTRACT NUMBER

5b. GRANT NUMBER

5c. PROGRAM ELEMENT NUMBER

5d. PROJECT NUMBER

5e. TASK NUMBER

5f. WORK UNIT NUMBER

6. AUTHORS

Carlos M. Torres Jr.
Alexandru Hening
Melvin Pascoguin
James R. Adleman
NIWC Pacific

7. PERFORMING ORGANIZATION NAME(S) AND ADDRESS(ES)

NIWC Pacific
53560 Hull Street
San Diego, CA 92152–5001

8. PERFORMING ORGANIZATION REPORT NUMBER

TR-3337

9. SPONSORING/MONITORING AGENCY NAME(S) AND ADDRESS(ES)

Office of Naval Research
One Liberty Center
875 N. Randolph Street
Arlington, VA 22203-1995

Naval Innovative Science and Engineering
53560 Hull Street
San Diego, CA 92152-5001

10. SPONSOR/MONITOR'S ACRONYM(S)

ONR/NISE

11. SPONSOR/MONITOR'S REPORT NUMBER(S)

12. DISTRIBUTION/AVAILABILITY STATEMENT

Approved for public release. Distribution is unlimited.

13. SUPPLEMENTARY NOTES

14. ABSTRACT

This technical report summarizes the work executed during FY21–FY23 of the Office of Naval Research (ONR)-funded Electrically-Tunable On-Demand Energy Bandstructures in Pulse Laser Deposited 2D Quantum Material Heterostructure-Based Devices (Qu-PLD) project and during FY21–FY22 of the Naval Information Warfare Center (NIWC) Pacific Naval Innovative Science and Engineering (NISE)-funded Quantum Engineered Nanodevices Exploiting Twistronics for Electromagnetic Maneuver Warfare (EMW) and Command, Control, Communications, Computers, Intelligence, Surveillance, and Reconnaissance (C4ISR) project. Most of the work was performed by NIWC Pacific scientists and engineers in the Quantum Engineered Nano Devices Laboratory (QENDL) at NIWC Pacific in San Diego, CA.

15. SUBJECT TERMS

Pulsed laser deposition (PLD); quantum materials; nanotechnology; 2D materials; 2D semiconductors; transition metal dichalcogenides (TMDs); cryogenic photoluminescence spectroscopy; direct bandgap modulation; excitons.

16. SECURITY CLASSIFICATION OF:			17. LIMITATION OF ABSTRACT	18. NUMBER OF PAGES	19a. NAME OF RESPONSIBLE PERSON
a. REPORT	b. ABSTRACT	c. THIS PAGE			Carlos M. Torres Jr.
U	U	U	SAR	40	19b. TELEPHONE NUMBER *(Include area code)* (619) 553-1614

This page is intentionally blank.

This page is intentionally blank.

Approved for public release. Distribution is unlimited.

Naval Information Warfare Center (NIWC) Pacific
San Diego, CA 92152-5001